Trapping, Detection, and Mass Measurement of Individual Ions in a Fourier Transform Ion Cyclotron Resonance Mass Spectrometer

J. E. Bruce, X. Cheng, R. Bakhtiar, Q. Wu, S. A. Hofstadler, G. A. Anderson, and R. D. Smith*

Contribution from the Molecular Science Research Center and Chemical Sciences Department, Pacific Northwest Laboratory, Richland, Washington 99352

Received February 21, 1994. Revised Manuscript Received June 14, 1994®

Abstract: A Fourier transform ion cyclotron resonance (FTICR) mass spectrometer has been used to trap *individual* multiply charged ions of several high molecular weight polymers, including poly(ethylene oxide), sodium poly(styrene sulfonate), and the protein bovine serum albumin. Detection of these ions is performed with the nondestructive method distinctive of FTICR, which also allows remeasurement of the same ion or ion population over several hours. For the determination of the charge states (and hence the masses) of individual ions, a new scheme was developed on the basis of the observation of the stepwise *m/z* shifts that result from charge exchange reactions or adduction of a substance of known mass. A novel technique for mass determination of individual ions has been made possible with the observation of cyclotron frequency shifts during the time-domain acquisition period. This time-resolved ion correlation (TRIC) technique allows reactant and product ions to be correlated with confidence and provides the basis for simultaneously studying a moderate number of ions. In this work, a range of observations related to the detection and measurement of individual ions is presented, as are examples of mass determinations of individual ions performed by utilizing the TRIC technique. Results are presented that show the measurement of poly(ethylene glycol) (PEG) individual ions of more than 5 MDa with more than 2500 net charges and measurement of ions as small as albumin (66 kDa) with as few as 30 charges. Other results illustrate that unexpected behavior can be observed for individual ions that would not be apparent in large ion populations.

Introduction

Since its introduction in 1984,[1] electrospray ionization (ESI) combined with mass spectrometry has undergone explosive growth,[2-4] not only as an analytical technique for molecular weight (MW) determination[2] but as a tool to probe fundamental aspects of ion formation,[5,6] protein structure and sequence,[7-10] and ion–molecule reactions.[11,12] Electrospray ionization has several attractive features that distinguish it from other ionization methods, including the ability to produce highly charged molecular ions from solution and efficiently ionize a wide range of molecules with molecular weights ranging from <100 Da to >5 MDa. The multiple charging phenomenon inherent to the ESI process is advantageous in that it produces relatively low mass-to-charge ratio (*m/z*) ions amenable to analysis by mass spectrometers with limited *m/z* ranges, such as quadrupole mass filters. Additionally, the production of a distribution of molecular ion charge states can yield a significant improvement in mass measurement accuracy.[13] ESI has been coupled to a wide range of mass spectrometers including quadrupole,[2] time-of-flight,[14] hybrid,[15] magnetic sector,[16] quadrupole ion trap,[17] and Fourier transform ion cyclotron resonance (FTICR) mass spectrometers.[18-20] Recent results obtained with the ESI–FTICR combination suggest it may be the ideal platform for the mass spectrometric study of large molecules based upon the demonstrated capability for ultra-high resolution and precision mass measurements,[21,22] the compatibility with on-line separations,[23] and the nondestructive detection scheme (which facilitates ion remeasurement[24-26] and multiple stage mass spectrometry, or $(MS)^n$, experiments[27]).

The FTICR detection method relies on the amplification of an image current produced by ion(s) undergoing cyclotron motion

* Corresponding author.

® Abstract published in *Advance ACS Abstracts,* July 15, 1994.

(1) Yamashita, M.; Fenn, J. B. *J. Phys. Chem.* **1984**, *88*, 4451–4459.
(2) Smith, R. D.; Loo, J. A.; Loo, R. R. O.; Busman, M.; Udseth, H. R. *Mass Spectrom. Rev.* **1991**, *10*, 359–451.
(3) Hamdan, M.; Curcuruto, O. *Int. J. Mass Spectrom. Ion Processes* **1991**, *108*, 93–113.
(4) Edmonds, C. G.; Smith, R. D. In *Methods in Enzymology: Mass Spectrometry*; McCloskey, J. A., Ed.; Academic Press: San Diego, CA, 1990; Vol. 193, pp 412–431.
(5) Fenn, J. B. *J. Am. Soc. Mass Spectrom.* **1993**, *4*, 524–535.
(6) Cole, R. B.; Harrata, A. K. *J. Am. Soc. Mass Spectrom.* **1993**, *4*, 546–556.
(7) Chowdhury, S. K.; Katta, V.; Chait, B. T. *J. Am. Chem. Soc.* **1990**, *112*, 9012–9013.
(8) Suckau, D.; Shi, Y.; Beu, S. C.; Senko, M. W.; Quinn, J. P.; Wampler, F. M.; McLafferty, F. W. *Proc. Natl. Acad. Sci. U.S.A.* **1993**, *90*, 790–793.
(9) Winger, B. E.; Light-Wahl, K. J.; Rockwood, A. L.; Smith, R. D. *J. Am. Chem. Soc.* **1992**, *114*, 5897–5898.
(10) Barinaga, C. J.; Edmonds, C. G.; Udseth, H. R.; Smith, R. D. *Rapid Commun. Mass Spectrom.* **1989**, *3*, 160–164.
(11) McLuckey, S. A.; Van Berkel, G. J.; Glish, G. L. *J. Am. Chem. Soc.* **1990**, *112*, 5668–5670.
(12) Loo, R. R. O.; Loo, J. A.; Udseth, H. R.; Fulton, J. L.; Smith, R. D. *Rapid Commun. Mass Spectrom.* **1992**, *6*, 159–165.
(13) Mann, M.; Meng, C. K.; Fenn, J. B. *Anal. Chem.* **1989**, *61*, 1702–1708.
(14) Boyle, J. G.; Whitehouse, C. M. *Anal. Chem.* **1992**, *64*, 2084–2089.
(15) Michael, S. M.; Chien, B. M.; Lubman, D. M. *Anal. Chem.* **1993**, *65*, 2614–2620.
(16) Allen, M. H.; Lewis, I. A. S. *Rapid Commun. Mass Spectrom.* **1989**, *3*, 255–258.
(17) Van Berkel, G. J.; McLuckey, S. A.; Glish, G. L. *Anal. Chem.* **1991**, *63*, 1098–1109.
(18) Henry, K. D.; Williams, E. R.; Wang, B. H.; McLafferty, F. W.; Shabanowitz, J.; Hunt, D. F. *Proc. Natl. Acad. Sci. U.S.A.* **1989**, *86*, 9075–9078.
(19) Hofstadler, S. A.; Laude, D. A. *Anal. Chem.* **1992**, *64*, 569–572.
(20) Winger, B. E.; Hofstadler, S. A.; Bruce, J. E.; Udseth, H. R.; Smith, R. D. *J. Am. Soc. Mass Spectrom.* **1993**, *4*, 566–577.
(21) Bruce, J. E.; Anderson, G. A.; Hofstadler, S. A.; Winger, B. E.; Smith, R. D. *Rapid Commun. Mass Spectrom.* **1993**, *7*, 700–703.
(22) Beu, S. C.; Senko, M. W.; Quinn, J. P.; McLafferty, F. W. *J. Am. Soc. Mass Spectrom.* **1993**, *4*, 190–192.
(23) Hofstadler, S. A.; Wahl, J. H.; Bruce, J. E.; Smith, R. D. *J. Am. Chem. Soc.* **1993**, *115*, 6983–6984.
(24) Williams, E. R.; Henry, K. D.; McLafferty, J. W. *J. Am. Chem. Soc.* **1990**, *112*, 6157–6162.
(25) Guan, Z. Q.; Hofstadler, S. A.; Laude, D. A. *Anal. Chem.* **1993**, *65*, 1588–1593.
(26) Speir, J. P.; Gorman, G. S.; Pitsenberger, C. C.; Turner, C. A.; Wang, P. P.; Amster, I. J. *Anal. Chem.* **1993**, *65*, 1746–1752.
(27) Senko, M. W.; Beu, S. C.; McLafferty, F. W. *J. Am. Soc. Mass Spectrom.* **1993**, *4*, 828–830.

0002-7863/94/1516-7839$04.50/0

in the confines of the trapped ion cell.[28] This nondestructive detection scheme permits the study of ions proceeding through one or more reaction steps, i.e. $(MS)^n$, and is used most effectively for structural studies based upon collisionally induced dissociation. As recently demonstrated, FTICR sensitivity can be greatly improved by multiple excitations and remeasurements of the same ion population[24-26] owing to the fact that the signal-to-noise ratio (S/N) is directly related to the square root of the number of scans coadded. S/N, and thus sensitivity, in FTICR is a function of several factors including ion cloud radius, number of charges in the ion ensemble, signal acquisition duration, transient decay rate, magnetic field strength, and the characteristics of the employed external amplification circuitry.[28] Marshall and co-workers[29] have obtained a detection limit of 177 singly charged ions with a S/N of 3:1 in a 3-T system utilizing a 1-s transient acquisition.

Several researchers have reported that ESI can produce molecular ions of species in the megadalton (MDa) mass range which produce signals detectable by standard quadrupole instrumentation.[30,31] In the recent work by Nohmi and Fenn,[30] a PEG sample with a nominal MW of 5 MDa produced a broad envelope of ions centered around m/z 1200 which was attributed to the unresolved mass and charge state distributions of the intact polymers. Assuming the large PEG ions are indeed intact, each individual molecule must have on the order of 4000 charges! Alternatively, a recent report by Xu et al.[32] suggests that large PEG molecular ions are unstable under electrospray conditions, undergoing dissociation to form much smaller ions. According to the recent study by Marshall and co-workers,[29] in their 3-T system, 4000 charges observed for 1 s should produce a frequency domain spectrum with a signal-to-noise ratio in excess of 65:1. Thus, *if* such a molecular ion can be successfully injected into and confined in the trapped ion cell, it should be feasible to accurately measure the mass-to-charge ratio of an *individual* ion.

It is important to point out that current ESI–MS methods have not been effective for molecules with MWs exceeding approximately 100–200 kDa. Due to the compression of mass information into a finite m/z range and the limited resolution of conventional ESI mass spectra, various algorithms are generally applied to mass spectra consisting of multiple charge state distributions to determine the charge state and, hence, the mass of the analyte. High-resolution ESI–FTICR spectra do not typically require the use of such algorithms since the charge state can be obtained directly from resolution of the 1-Da isotopic spacing. In fact, the resolution readily achievable with FTICR would lead one to believe that the charge states for species with MWs exceeding 10^6 Da should be obtainable and, thus, the analysis of compounds with extremely high MWs should pose no significant problem. Unfortunately, the extrapolation to very large, highly charged molecules fails due to factors that include greatly increased sample heterogeneity. Other limitations arise due to practical limitations upon sample size and stochastic limitations from the finite charge storage capacity of the FTICR trapped ion cell. Thus, for the analysis of increasingly large molecules by ESI–FTICR, conventional methods that rely on the detection of large ensembles of ions and distinct charge states or resolution sufficient to measure isotopic spacings ultimately prove inadequate. An approach to large ion measurements based on the detection of individual ions can potentially overcome these limitations. Individual ion charge (and mass) can be obtained by the observation of reaction processes that produce a change in ion charge (charge state shifts) or mass (addition/dissociation of neutrals of known mass).

Single (i.e., "individual") molecule detection has been the focus of efforts to improve the sensitivity of many analytical techniques.[33] For example, the ability to image single molecules using optical and near-field optical microscopic and spectroscopic techniques has been demonstrated[34] and used to directly observe individual molecules of *Estericha coli* RNA polymerase as they translocate along immobilized bacteriophage T7 DNA.[35] Additionally, using laser excited fluorescence, Whitten and co-workers[36] achieved single molecule detection limits for fluorescent compounds dissolved in macroscopic glycerol–water droplets. In the study of ion–ion interactions and in ultraprecise mass measurements, very specific detection methods have been developed on the basis of ion-trapping techniques which utilize electrodynamic[36] and Penning[37] ion traps. Single ion cyclotron resonance (SICR) measurements with Penning traps[38] have demonstrated extremely precise mass determinations for small ions such as CO^+ and N_2^+ in the absence of the Coulombic effects present when multiple ions are trapped. The detection of individual ions with unit charge was made possible only with the implementation of a narrow-band tuned detection circuit,[39] and, hence, presents obvious limitations as a general detection scheme.

In this work, we expand on our initial report,[40] which described the first trapping, detection, and measurement of individual ions, and we present results showing that individual ions having molecular weights ranging from ~66 kDa to >5 MDa can be successfully ionized, injected, trapped, and detected using ESI–FTICR. We also show that the MWs of individual ions can be determined by the observation of peak shifting due to reactions that induce changes in charge states. The new methods developed for this work are described, a range of the phenomena encountered is presented, and the potential utility and extension of these methods are discussed.

Experimental Section

All experiments were performed with a 7-T external source FTICR mass spectrometer equipped with a modified Analytica (Analytica, Branford, CT) electrospray ionization source described in detail elsewhere.[20] Pulse sequence timing and electronics were controlled by an IonSpec (Irvine, CA) Omega data station. The initial individual ion experiments used the synthetic polymer poly(ethylene oxide) (Sigma, St. Louis, MO), commonly referred to as poly(ethylene glycol) or PEG, with a nominal molecular weight of 5×10^6 Da. The limits of detection of the individual ion experiments were determined with various polymers ranging in size from 5 MDa to 66 kDa and included various PEG molecules (nominal MWs 600 kDa and 5 MDa), sodium poly(styrene sulfonate) (PSS) molecules (nominal MWs 177 kDa and 1.06 MDa), bovine albumin dimer (MW 133 kDa), and bovine albumin (MW 66 kDa). Proteins were prepared as solutions with concentrations of 0.5–1.0 mg/mL in 25:75 $CH_3OH/(5\%\ CH_3COOH/H_2O)$ and were obtained in the positive ion mode to generate multiply protonated ions. PSS solutions were 1.0 mg/mL in 50:50 CH_3OH/H_2O, and PEG solutions were 1–100 μg/mL in 50:50 CH_3OH/H_2O and 1 mM NaCl. All samples were infused at 0.5 μL/min. PSS and PEG electrospray spectra resulted from Na^+ detachment (negative ion mode) and adduction (positive ion mode), respectively.

Experimental parameters employed for trapping and detection of large individual ions were similar in many respects to those used for previous studies involving populations of lower molecular weight ions. An exception

(28) Comisarow, M. B. *Anal. Chim. Acta* **1985**, *178*, 1–15.
(29) Limbach, P. A.; Grosshans, P. B.; Marshall, A. G. *Anal. Chem.* **1993**, *65*, 135–140.
(30) Nohmi, T.; Fenn, J. B. *J. Am. Chem. Soc.* **1992**, *114*, 3241–3246.
(31) Edmonds, C. G.; Springer, D. L.; Morris, B. J.; Thrall, B. D.; Camp, D. G. Proceedings of the *41st ASMS Conference on Mass Spectrometry and Allied Topics*; ASMS: Washington, DC, 1993; pp 272a–272b.
(32) Xu, Y.; Bae, Y. K.; Beuleher, R. J.; Friedman, L. *J. Phys. Chem.* **1993**, *97*, 11883–11886.
(33) Kopelman, R.; Tan, W. *Science* **1993**, *262*, 1382–1384.
(34) Betzig, E.; Chichester, R. J. *Science* **1993**, *262*, 1422–1425.
(35) Kabata, H.; Kurosawa, O.; Arai, I.; Washizu, M.; Margarson, S. A.; Glass, R. E.; Shimamoto, N. *Science* **1993**, *262*, 1561–1563.
(36) Whitten, W. B.; Ramsey, J. M. *Anal. Chem.* **1991**, *63*, 1027–1031.
(37) Brown, L. S.; Gabrielse, G. *Rev. Mod. Phys.* **1986**, *58*, 233–311.
(38) Cornell, E. A.; Weisskoff, R. M.; Boyce, K. R.; Flanagan, R. W., Jr.; Lafyatis, G. P.; Pritchard, D. E. *Phys. Rev. Lett.* **1989**, *63*, 1674–1677.
(39) Weisskoff, R. M.; Lafyatis, G. P.; Boyce, K. R.; Cornell, E. A.; Flanagan, R. W., Jr.; Pritchard, D. E. *J. Appl. Phys.* **1988**, *63*, 4599–4604.
(40) Smith, R. D.; Cheng, X.; Bruce, J. E.; Hofstadler, S. A.; Anderson, G. A. *Nature*, **1994**, *369*, 137–139.

was the additional events used for the separation of large individual ions from the more abundant lower MW species, discussed in detail later. The ICR cell employed for the present study was a 5- × 5- × 7.6-cm orthorhombic version mounted directly to the end of the quadrupole ion guide used for ion injection. Trapping potentials during the accumulation period were typically 4–5 V but were varied to match the measured kinetic energy of the injected ions. After the ion accumulation event (0.1–2 s) and a subsequent pump-down interval (10–60 s), the trapping potentials were reduced to 0.5–0.25 V for the detection period.

All extended time domain data sets were acquired with a separate 66-MHz 486 computer (Gateway 2000, N. Sioux City, SD) and digitizer (Model Number DT 2839, Data Translation, Marlboro, MA), similar to that described elsewhere.[21] Experiments performed to determine the limits of detection were typically performed with 256K data points acquired with an IonSpec Omega data station. All control pulses and excite pulses (with the exception of SWIFT waveforms) were provided by the IonSpec data station. The extended transient signals were digitized at 100 or 200 KHz in the broad-band mode and ranged in length from 256K to 16 384K data points. SWIFT waveforms,[41] when used for excitation and/or ejection, were designed with software written in our laboratory and were implemented with a LeCroy arbitrary waveform generator (LeCroy, Chestnut Ridge, NY). All software used to process and display transients and frequency domain spectra with the 486 computer was developed at this laboratory using published algorithms.[42] All calculations were performed with single precision floating point real numbers.

Results and Discussion

Several kinds of evidence were acquired to initially demonstrate that the detected signals did, in fact, arise from individual ions in the FTICR trap. Distinct differences were observed between the behaviors of individual macroions (i.e., >1 MDa) and larger populations of smaller ions (i.e., <100 000 Da), including longer suspended trapping lifetimes, discrete stepwise shifts in cyclotron frequency observed with successive remeasurements, and the observed signal dependence upon cyclotron excitation levels. The less abundant peaks detected and ascribed to individual ions can be readily distinguished from signals not originating from ion-induced currents (i.e., background or "correlated" noise peaks characteristic of the laboratory environment) in the observed mass spectrum by subtraction of appropriate background spectra and by observation of the frequency dependence of remeasured ion peaks on the applied trapping potential. As will be demonstrated, however, the most conclusive evidence for the ability to detect individual ions in the ICR cell comes from the time-resolved ion correlation (TRIC) technique we introduce here. This technique also provides the basis for the simultaneous study of many individual ions, a capability that should prove to be useful in practical applications.

In our studies, ions are transported from the atmospheric pressure ESI source to the trapped ion cell using two sets of rf-only quadrupoles and are trapped with the bias applied to the trapping electrodes appropriate for the kinetic energy of the injected ion beam. A relatively high pressure ($\sim 10^{-4}$ Torr) nitrogen gas pulse provides collisions needed for effective deceleration and confinement in the cell. Generally, longer gas pulses and higher pressures have been found more effective for trapping larger ions. Large ion populations trapped in this manner produced spectra similar to those reported earlier with quadrupole mass spectrometers[30] and do not directly yield molecular weight information due to the range of possible molecular weight species present in the large polymer samples, combined with isotopic dispersity and multiple charge states. From large populations of ions with variable sizes, we have found that individual ions with high molecular weights can be readily isolated.

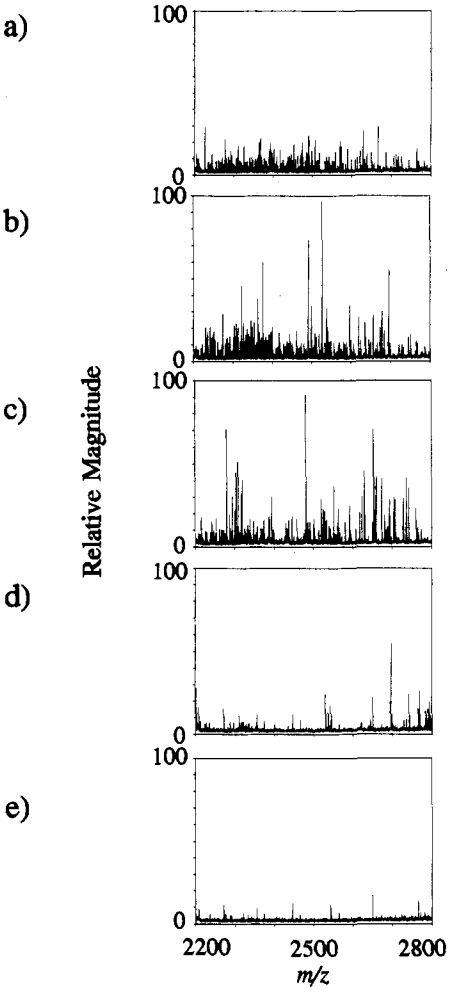

Figure 1. Successive mass spectra of multiply charged PEG ions illustrating the observed effect of mass discrimination upon increasing excitation rf amplitude. All parameters used to acquire the following spectra were held constant with the exception of rf excitation voltage: (a) rf(excite) = $40V_{pp}$, (b) rf(excite) = $56V_{pp}$, (c) rf(excite) = $65V_{pp}$, (d) rf(excite) = $104V_{pp}$, (e) rf(excite) = $150V_{pp}$.

Several techniques, based on suspended trapping[43-45] and the observed *m/z* dependence of excitation amplitude,[46] have been employed to discriminate against lower molecular weight species. Our initial communication demonstrated the use of suspended trapping for discrimination against species of lower mass but similar *m/z* and showed that for longer suspensions of trapping voltages (>50 ms) the ion population for 5-MDa PEG ions could also be reduced so that only a few ions, generally broadly spaced in *m/z*, remained in the cell.[40] Another approach to the isolation of large ions (that was not originally anticipated to be useful) was also demonstrated upon the basis of the different behavior upon excitation. Our studies of large individual ions have indicated that proper selection of excitation conditions is necessary to obtain optimum sensitivity and that the excitation process itself could also be effective for selective isolation of higher molecular weight ions in the trap. The data shown in Figure 1a were obtained with a chirp excitation amplitude of $40V_{pp}$. A gradual increase in rf amplitude from $40V_{pp}$ to $150V_{pp}$, each time with a new population of ions, produced the spectra shown in Figure 1b–e. At $150V_{pp}$, no ion signal was detected and the observed peaks shown in Figure 1e define the background noise spectrum. As will be demon-

(41) Marshall, A. G.; Wang, T.-C. L.; Ricca, T. L. *J. Am Chem. Soc.* **1985**, *107*, 7893–7897.
(42) Press, W. H.; Teukolsky, S. A.; Vetterling, W. T.; Flannery, B. P. *Numerical Recipes in C. The Art of Scientific Computing*, 2nd ed.; Cambridge University Press: Cambridge, U.K., 1988.
(43) Laude, D. A., Jr.; Beu, S. C. *Anal. Chem.* **1989**, *61*, 2422–2427.
(44) Hogan, J. D.; Laude, D. A., Jr. *J. Am. Soc. Mass Spectrom.* **1990**, *1*, 431–439.
(45) Dunbar, R. C.; Weddle, G. H. *J. Phys. Chem.* **1988**, *92*, 5706–5709.
(46) Huang, S. K.; Rempel, D. L.; Gross, M. L. *Int. J. Mass Spectrom. Ion Processes* **1986**, *72*, 15–31.

strated, the peaks in Figure 1d correspond to large, highly charged individual ions. The more abundant ions that are ejected at higher rf levels (compare Figure 1c,d) may be attributed to lower molecular weight species. Thus, the excitation amplitude dependence in conjunction with SWIFT isolation of a range of m/z values was used as a technique to remove the unwanted, presumably lower molecular weight, species and to reduce the ion population to a more manageable number (typically 1–100 ions). The observed difference in behavior upon excitation between small and large ions of similar m/z is possibly a result of the more rapid growth of magnetron motion for smaller ions due to collisional processes. A substantial displacement from the cell axis due to magnetron motion would result in ejection of lighter ions from the cell at lower rf excitation levels. Also consistent with this explanation is the observation that extended trapping periods with elevated pressures favor retention of heavier ions in the cell, presumably due to more rapid growth of the magnetron radius for lighter ions.

In the present TRIC studies, a SWIFT waveform was created which was used to eject all ions from the trapped ion cell except for those residing in a very narrow m/z range; these ions were excited to radii appropriate for the detection of large individual ions. The nonejection band varied in width from 5 to 100 m/z units and was generally selected to be in the m/z region having the greatest population of trapped ions. As shown in our earlier communication,[40] nearly comparable results can be obtained by suspension of trapping voltages for various time periods and, depending upon the desired result, either with or without the use of subsequent ion ejection techniques.

The TRIC technique was developed to more effectively examine the time dependence of weak individual ion signals and to establish a time-resolved link between reactant and product ions. Figure 2 illustrates the basis of the TRIC technique in which ion A reacts to form ion B, which in turn reacts to form ion C. The entire transient (upper left) includes the cyclotron frequency range of the individual ions A, B, and C. To the right of this transient is shown the result of Fourier transformation of this signal, or the frequency domain spectrum. Note that all three ions appear in this spectrum with differing amplitudes. For conventional FTICR experiments involving three populations of ions, the differences in frequency domain amplitudes would reflect the size of the three ion populations, and possibly differing cyclotron radii, contributions due to reactive loss, loss of phase coherence, and possible differences in damping rates. However, for individual ion studies, this is not the case; individual ion peak magnitudes are related to charge, cyclotron orbit radii, damping rate, and ion lifetime. Initial isolation of an individual ion provides a unique situation where a reaction process can lead to an abrupt change in peak position, i.e. one cyclotron frequency disappears simultaneous with the appearance of another. The TRIC technique relies on the production of individual time-domain signals to follow reaction processes for each ion observed. One way in which this is accomplished in the present work is by first forcing the amplitude of the real and the imaginary components of the entire frequency-domain spectrum to zero, with the exception of the frequency bandwidth(s) of interest, i.e. a narrow range about A, B, and C. The resulting spectrum is called a selected frequency-domain spectrum. The inverse transformation of the resultant selected frequency-domain spectrum (both real and imaginary components) is then used to produce a time-domain signal of the selected frequency range, *with its temporal fluctuations intact*. The result is a "real-time" record of the behavior of each of the selected ions, documenting any reactive processes that occur during the transient. Comparison of several individual ion time-domain signals extracted from a single transient generally allows a correlation between the appearance and disappearance of individual ions to be constructed. This is possible even when numerous ions are simultaneously present due to differences in

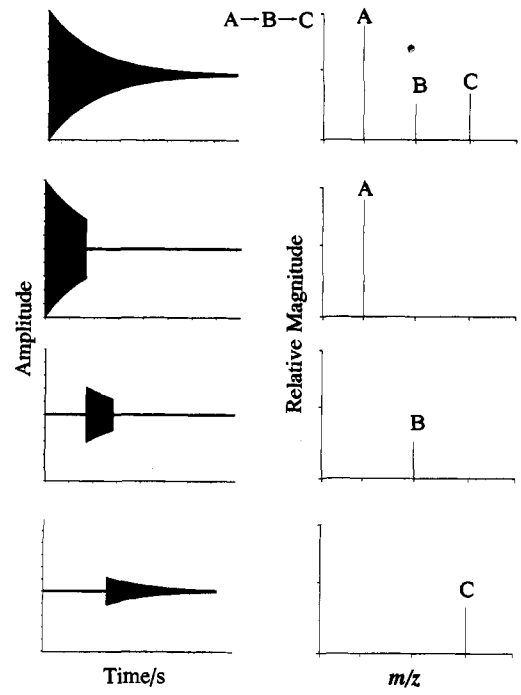

Figure 2. Schematic diagram illustrating the basis of the time resolved ion correlation (TRIC) analysis technique. All individual ion signals are first simultaneously recorded and processed, as in conventional FTICR procedures. Next, m/z or frequency-domain regions encompassing the observed peaks are chosen and windowed with a function that forces to zero the amplitude of the remainder of the spectrum. Inverse Fourier transformation of the resulting selected frequency-domain spectrum produces the time-domain signal corresponding to the selected frequency range, with temporal variations intact. Comparison between various selected frequency time domain signals allows a correlation of the reactant and product relationship for individual ions undergoing discrete shifts in m/z due to their simultaneous disappearance and appearance.

m/z (since large ion transitions are generally restricted to a relatively small m/z region of the spectrum) and the temporal signature provided by the TRIC analysis. Thus, with the examination of the individual time-domain signals afforded by TRIC, the reactive path A → B → C becomes evident.

The discrete temporal behavior of ions is key to establishing that they are in fact individual ions. The TRIC analysis will not produce similar information for ensembles of ions as the reaction of an ensemble of ions of a given m/z occurs at a distribution of times resulting in a loss of coherence and a gradual decrease in precursor ion signal with no detectable product ion signal. The differences in amplitude shown in the full frequency domain spectrum in Figure 2 arise due to differing ion cyclotron radii and differing ion lifetimes, as is evident from the extracted time-domain signals of ions A, B, and C. In addition to correlating reactant and product ions, the TRIC analysis provides an effective basis for mass measurements of individual ions by observation of their reactions, provided that the shifts from A to B to C arise from reaction processes causing a known mass change and/or charge shift. For ions of two different masses, m_a and m_b, and charges, z_a and z_b, with mass-to-charge ratios, m_a/z_a $(=(m/z)_a)$ and m_b/z_b, we need to determine four unknowns, m_a, m_b, z_a, and z_b, in order to determine the mass of the ion and the neutral molecular species, M, from which each ion is derived. For ions that are all produced by cation or anion attachment with the same neutral mass, M, the general equation

$$(m/z)_i = \frac{M + n_i(m_{cc})}{n_i(z_{cc})} \qquad (1)$$

is true, where n_i, m_{cc}, and z_{cc}, are the number of charge carriers,

the mass of each charge carrier, and the charge of each charge carrier, respectively. Rearrangement to solve for the number of charges yields

$$n_i = \frac{M}{(m/z)_i z_{cc} - m_{cc}} \tag{2}$$

For mass spectra derived from cation or anion attached species, such as electrospray spectra, any two peaks, $(m/z)_a$ and $(m/z)_b$, of a given series are separated by an integer number of charges, Δ, so

$$n_a - \Delta = n_b \tag{3}$$

Writing eq 2 in terms of the two ions, $(m/z)_a$ and $(m/z)_b$, yields

$$\Delta(z_{cc}) = \frac{M + n_a(m_{cc})}{(m/z)_a} - \frac{M + (n_a - \Delta)(m_{cc})}{(m/z)_b} \tag{4a}$$

or alternatively

$$\frac{M}{(m/z)_a z_{cc} - m_{cc}} - \Delta = \frac{M}{(m/z)_b z_{cc} - m_{cc}} \tag{4b}$$

Solving eq 4 for M gives

$$M = \Delta\left\{\frac{[(m/z)_a - (m/z)_{cc}][(m/z)_b - (m/z)_{cc}]}{|(m/z)_b - (m/z)_a|}\right\} \tag{5}$$

If the observed peaks represent different charge states of the same species, eq 5 can be used to calculate M for an ion that has undergone charge exchange from $(m/z)_a$ to $(m/z)_b$, where m_{cc} and z_{cc} are the mass and charge (commonly ± 1) of the charge carrier and Δ is the difference in charge state between the peaks at $(m/z)_a$ and $(m/z)_b$. If many consecutive shifts are observed, the series of charge states may be analyzed using various techniques, resulting in considerably reduced errors in the molecular weight determination. Similarly, eq 6 can be used to calculate the molecular weight of an ion that has undergone adduction from $(m/z)_a$ with a known neutral mass (N) to form $(m/z)_b$ without changing the charge, z.

$$M = \frac{N[(m/z)_a - (m/z)_{cc}]}{|(m/z)_b - (m/z)_a|} \tag{6}$$

Several extended time-domain data sets were acquired for the PEG samples following selection of individual ions from the initially dense envelope of trapped ions, as described earlier. Typical raw time-domain signals for a limited number of ions, acquired at 100 or 200 KHz in the broad-band mode, showed no appreciable signal above that of the background noise level, as might be expected for the relatively weak individual ion signals. However, Fourier transformation produced useful frequency domain signals of individual ions, as shown by the spectrum in Figure 3. These data were acquired with a 50 m/z acceptance window SWIFT waveform, centered at m/z 2500. As shall be demonstrated, the signal shown in Figure 3 resulted from trapping several individual ions. The peak splitting apparent in this spectrum (and in Figure 5 (bottom)) results from gradual (physical) frequency shifting over relatively long time intervals, arising due to the damping of cyclotron motion and the nonideal fields that apply for our cell, as has been previously observed for smaller molecules.[21,47] A TRIC analysis allows the time dependence of these signals, as well as the relationships between

(47) Guan, S. H.; Wahl, M. C.; Marshall, A. G. *Anal. Chem.* **1993**, *65*, 3647–3653.

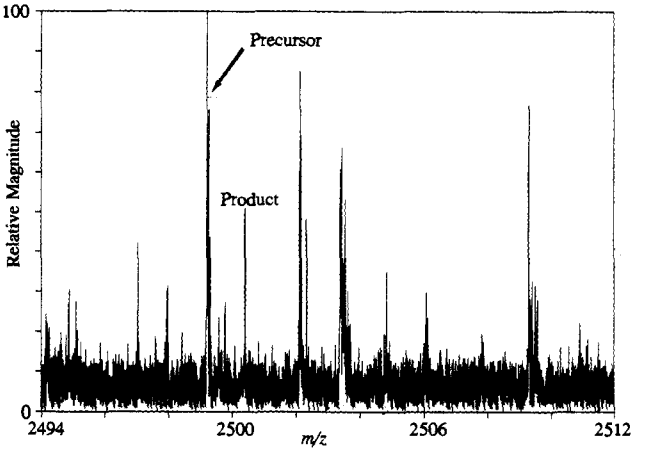

Figure 3. Mass spectrum of several individual PEG ions isolated with a SWIFT waveform with a 50 m/z acceptance window. The relationship between precursor and product ion is further illustrated with extracted time-domain signals in Figure 4.

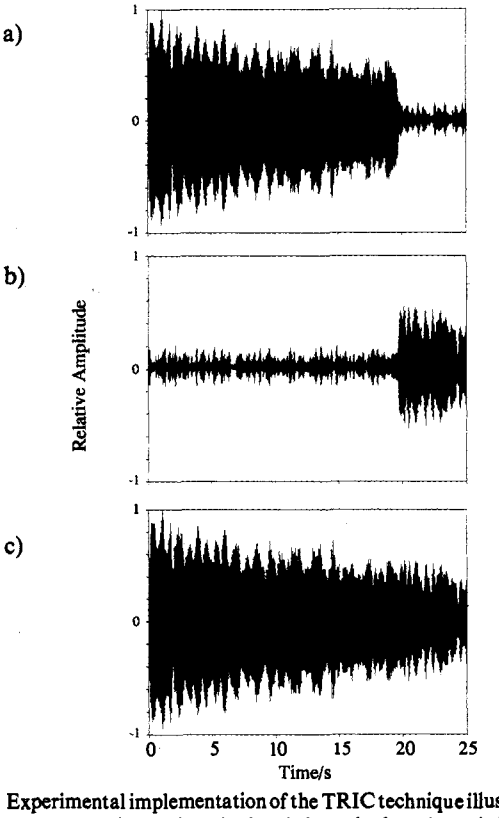

Figure 4. Experimental implementation of the TRIC technique illustrated with frequency-selected time-domain signals from the data shown in Figure 3. The frequency ranges extracted correspond to 0.5 m/z windows about (a) m/z 2499.3 and (b) m/z 2500.7. (c) Superposition of the two extracted time-domain signals shown in a and b.

these peaks to be clearly defined. Figure 4a,b show the selected time domain waveforms produced by extracting the relevant narrow frequency ranges (corresponding to 0.5 m/z) from the full frequency-domain spectrum followed by inverse Fourier transformation. This figure clearly establishes the temporal relationship between the precursor ion at m/z 2499.3 (a) and the product ion at m/z 2500.4 (b). This relationship was presumably produced by charge loss (most likely Na^+) from PEG molecular ions due to collisions with background species and yields a molecular weight of 5.4×10^6 Da using eq 5. Figure 4c shows the superposition of the two extracted time-domain signals.

In the course of many similar experiments, we observed several cases showing unexpected phenomena. Figure 5 (top) gives the spectrum from another similar experiment involving the observa-

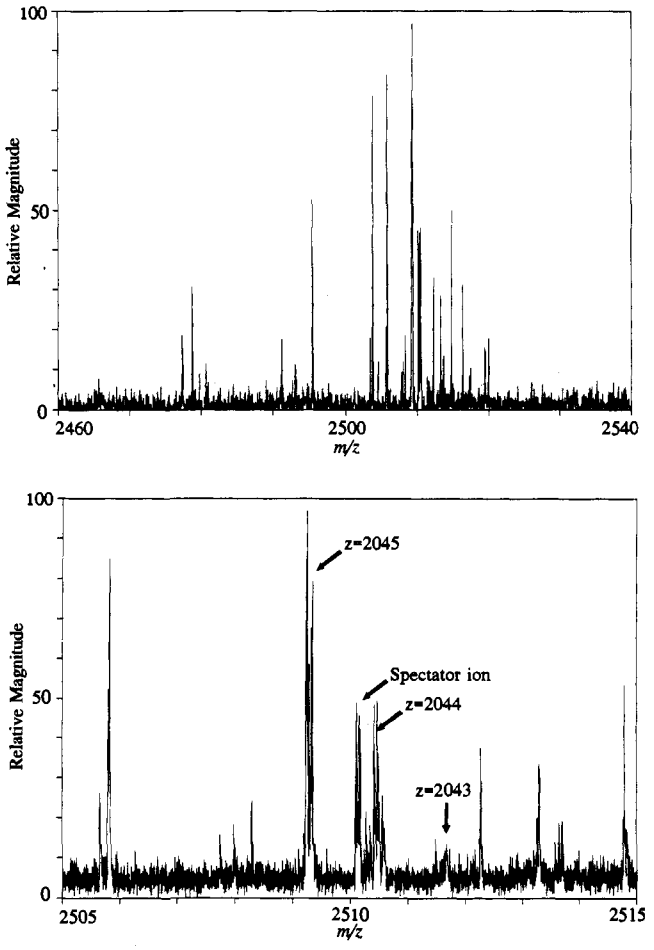

Figure 5. (top) Mass spectrum of many individual ions obtained with a SWIFT waveform retaining the range from 2475 to 2525 *m/z*. (bottom) Selected *m/z* mass spectrum illustrating the region in which multiple charge state shifting events involving the ions near *m/z* 2510 were observed.

tions of PEG ions following their selection and excitation with a SWIFT waveform with a 50 *m/z* acceptance window centered at 2500 *m/z*. Figure 5 (bottom) shows an expansion of the *m/z* region in which multiple charge state shifting events involving the ions near *m/z* 2510 were found to occur. With standard data processing techniques, i.e. Fourier transformation of the time-domain signal and subsequent presentation of the magnitude mode spectrum, the charge shifting of these ions, which will become plainly evident later, is not revealed. The TRIC analysis of these data showed a correlation between the appearance and disappearance of several of these ions, ion A = *m/z* 2509.25, ion B = *m/z* 2510.45, and ion C = *m/z* 2511.70 (barely visible in the full spectrum due to its limited lifetime and reduced cyclotron radius). Also observed was the absence of interaction of the ion at *m/z* 2510.19, which we describe as a *spectator ion*, since this ion does not react, but merely "watches" the reactions linking A, B, and C. The spectator ion is readily distinguished from those peaks due to "correlated noise" by its distinctive signal damping due to a gradual reduction in cyclotron radius and the small related "physical shift" in cyclotron frequency. Furthermore, the area between *m/z* 2475 and 2525 was chosen for the present study due to the small contributions of correlated noise peaks in this region. The TRIC analysis of these ions is shown in Figure 6a–c, which gives their time-domain signals produced by inverse Fourier transformation of a 0.4 *m/z* window around ions A, B, and C. The combination of all of the above time-domain signals is illustrated in Figure 6d, demonstrating the extremely slow damping of cyclotron motion typically observed in our studies of these large molecules.

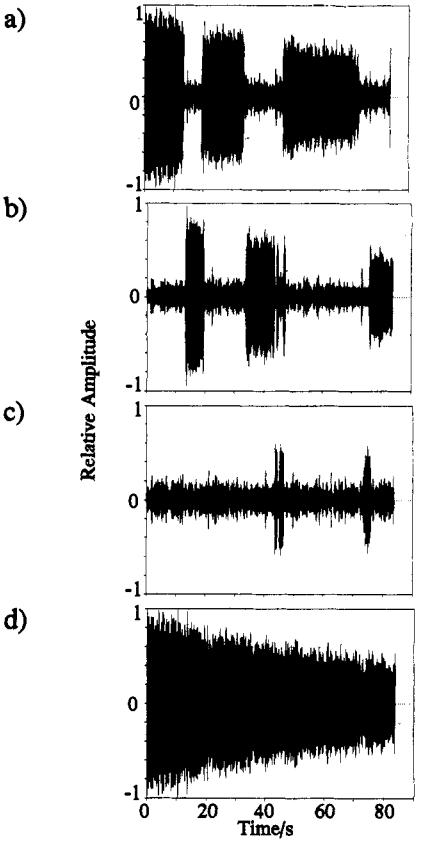

Figure 6. TRIC frequency-selected time-domain signals from the spectra shown in Figure 5. Frequency ranges extracted correspond to 0.4 *m/z* windows about the following *m/z* values: (a) 2509.25, (b) 2510.45, and (c) 2511.70. (d) Superposition of all of the time-domain signals shown in a, b, and c, demonstrating the extremely slow damping of cyclotron motion commonly observed in our studies of extremely high MW species.

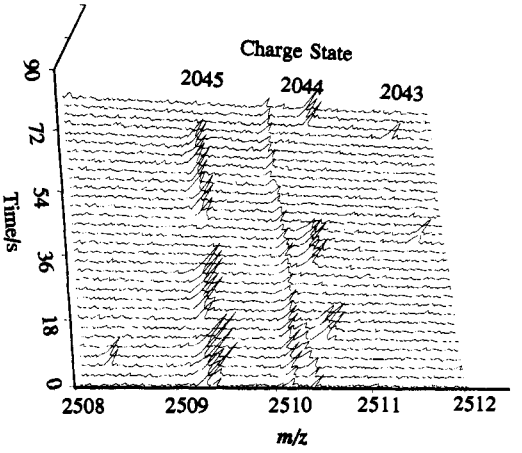

Figure 7. Stack plots produced by successive Fourier transformation to the frequency (*m/z*) domain of small segments of data across the entire raw time domain data set used to produce Figures 5 and 6.

The same data shown in the time-domain plots in Figure 6 can be portrayed in a stack plot version that further illustrates the relationships between all of the observed peaks. Figure 7 illustrates the results of successive Fourier transformation of small increments of data throughout the entire data set. The relationships between the three charge states are clearly shown in this figure; however, the actual time of the reaction is more uncertain (to an extent that depends on the size of the segment of data used to create each mass spectrum) than that produced with the time-domain plots of Figure 6. Furthermore, ions with short lifetimes, such as those due to the oscillations between charge states 2044

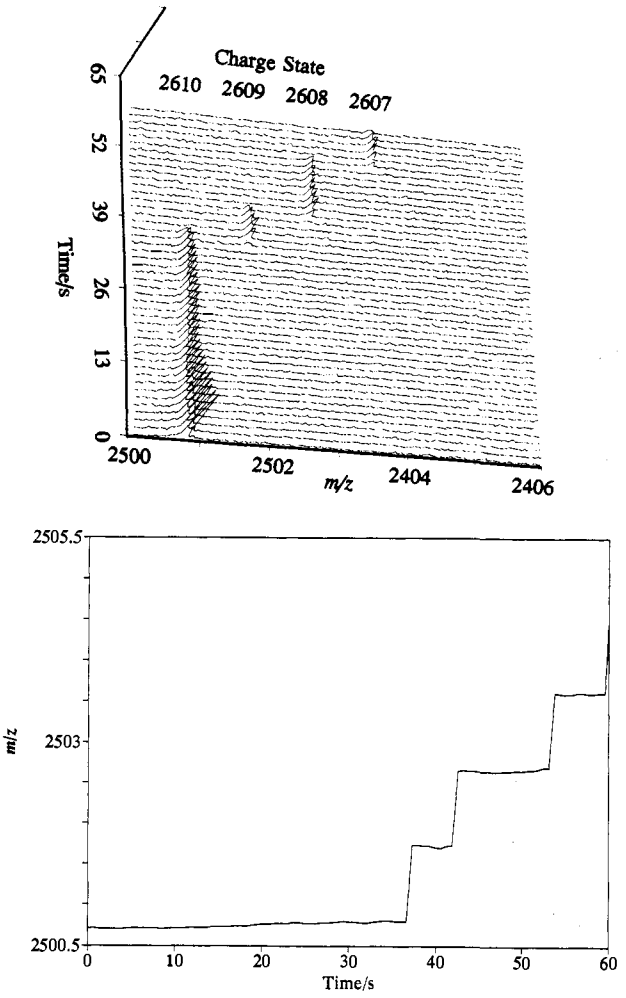

Figure 8. (top) Stack plots produced by successive Fourier transformation of small segments of data across the entire raw time-domain data set acquired with a single individual PEG ion. (bottom) *m/z* vs time plot illustrating the evolution of a single individual PEG ion as it undergoes charge loss steps during the acquisition of the time domain signal at times of approximately 38, 43, and 54 s.

and 2043 evident in Figure 6b,c around 47 s, are not effectively displayed with the stack plot approach, due to the finite data segment size requirement of the Fourier transform.

Similar TRIC analyses on single ion data from our earlier communication[40] is shown in Figure 8 to better illustrate the interesting chemistry of these large single PEG ions. These data show the detection of three consecutive charge shifts of a single individual PEG ion that was isolated and detected with a 5 *m/z* SWIFT isolation and detection window. The mass spectra of Figure 8 (top) clearly show the relationships correlating these ions. Since only one ion was detected in the mass spectrum at any given time, a *m/z* vs time plot could be generated by similar segmented Fourier transformation analysis, as was done for our previous investigations involving physical frequency shifting phenomenon.[21] These results also clearly illustrate the charge shifting behavior of the large PEG ions and are presented in Figure 8 (bottom) and show both the relatively large *m/z* shifts due to charge loss as well as the smaller gradual "physical shift".

All abrupt shifts in observed cyclotron frequency in the present examples are ascribed to charge state shifts. The observation that frequency shifts can occur in both directions (i.e., increase as well as decrease) in some cases (as evident in Figures 5–7) is extremely surprising, and may possibly be attributed to Na^+ detachment and reattachment or Na^+ transfer to and from small background neutrals. Na^+ ions lost (either as free ions or attached to background neutrals) from the multiply charged PEG ions might remain trapped in the ICR cell and have a finite possibility of reattachment to the large PEG ions. In order to do this, however, the ion would presumably have to surmount an appreciable Coulombic barrier. However, it seems feasible that a large stringlike structure of the PEG ion might also have regions of fairly low charge density and thus might not produce excessively high Coulombic repulsion with another small ion, and possibly facilitate Na^+ transfer or reattachment. Free Na^+ or small sodium cation attached species (resulting from Na^+ ion transfer to small background neutrals) would not be detected under the present conditions since the cyclotron frequency of these ions would be far beyond the detection bandwidth employed and the estimated signal magnitude for a single charge would be approximately 2000 times weaker than that of the PEG ions. Particularly surprising, however, is the observation that one ion gains and loses charge several times during the 80-s observation period while another ion appears completely unreactive. This suggests the possibility that the charge shifting might arise from reencounters of the large PEG ion with the same small charged species. An alternative explanation for our observations is that some other ion–neutral collision phenomena may occur that can result in formation of an additional charge site followed by separation of the new oppositely charged products, a process that is also viewed as unlikely under the employed conditions. While neither of these explanations is entirely satisfactory, the data (and several other examples from similar studies) indicate that both charge loss and charge gain steps are feasible. This is a striking observation, clearly demanding additional study.

Table 1. Molecular Mass Measurements Performed on Individual Ion Data Presented in Figures 7 and 8 Calculated with the Fit Charge States and Measured *m/z* Values Indicated[a,b]

charge state (fit)	*m/z* (measd)	MW
	Data from Figure 7	
2045	2509.292	5 084 488
2044	2510.508	5 084 487
2043	2511.651	5 084 334
	average MW =	5 084 436 ± 200
	Data from Figure 8	
2610	2500.707	6 466 842
2609	2501.723	6 467 015
2608	2502.648	6 466 949
2607	2503.610	6 466 977
	average MW =	6 466 946 ± 125

[a] The errors in molecular weight assume the fit charge states are correct and result from adducted Na^+ ions. [b] Error limits indicate the 95% confidence limits based on the presented molecular weight determinations.

The molecular weight of the individual ions studied that have undergone certain reaction processes can be ascertained using eqs 5 and/or 6. The observed *m/z* values of the two individual ion data sets illustrated above are presented in Table 1. All frequency shifts observed in the present PEG individual ion studies are assumed to arise due to Na^+ transfer. Consequently, the data were fit to a series of charge states and used to calculate the molecular weights presented in Table 1. Attempts to calculate molecular weights based on eq 6, assuming the adduction and/or loss of a neutral species, such as H_2O or N_2, resulted in molecular weights of 47 000 and 73 000, respectively, for the data shown in Figure 8. Electrospray spectra normally provide multiple molecular weight measurements for each spectrum due to the multiple analyte charge states. In individual ion studies, only one charge state or related peak is observed at any particular time during the transient. However, over the course of the transient, the individual ion reacts to form other charge states or adducted species and, therefore, allows several molecular weight measurements for the same molecule. These molecular weight measurements yield an average molecular mass (as reported above) but do not include any variation in composition of the species under observation (i.e., contributions due to heterogeneity)

since all determinations originate from the same molecule. As we noted in our initial communication,[40] measurements that account for heterogeneity, or that are reflective of a molecular weight for a sample, require that a number of individual ions be examined. However, if the molecular weight distribution arises only from isotopic heterogeneity, remarkably few ions for very large molecules need be measured to obtain precise measurements. For one ion, an average error estimate may also be produced from the multiple molecular mass measurements (just as if an object had been weighed several times) by comparison of the range of observed values with the average value. The calculations based on charge-transfer processes, assuming the fit charge states are correct, produce molecular weight measurements with an average error of ~20 ppm (95% confidence limits of the mean, $n = 4$). Assuming charge-transfer processes are the cause of the shifting cyclotron frequencies, comparison of the molecular weight measurements for the three individual ions studied shows them to be somewhat different. However, this difference is not unexpected for a sample that has a reported polydispersity of 1.2. A likely source of much of the encountered error is the physical frequency shifting (mentioned earlier) as well as contributions arising from small neutral adduction and loss. These phenomena are particularly evident upon the addition of a low pressure of various reagents to the cell and will be the subject of a future paper. Calculations based on eq 5 produce smaller errors with an average MW of 6 300 000 ± 800 000 (95% confidence limits of the mean, $n = 3$). Furthermore, fitting the series of peaks with a technique based on the reduction of both δ and $\delta(\delta)$, where δ is the average of the absolute difference between the calculated and measured m/z and $\delta(\delta)$ is the average of the absolute difference between consecutive δ's, results in significantly reduced errors. The resulting charge states fit and resulting mass determinations are presented in Table 1. The demands upon m/z measurement precision needed for confident assignment of the charge state increase in proportion with molecule mass. If insufficient measurement precision exists due to molecule size or few charge state shifts are observed, the mass precision becomes limited by the uncertainty in charge state assignment.

In an effort to determine the lowest molecular weight species that can be effectively detected with the present system, a series of molecules with varying molecular weights was analyzed and the resulting peaks were subjected to the same scrutiny as were those of the PEG ions (with the exception of the TRIC technique). The smallest molecule confidently detected as an individual, multiply charged ion with the present instrumentation was bovine albumin. We have measured signal-to-noise ratios (S/N) for bovine albumin (MW = 66.3 kDa), bovine albumin dimer (MW = 133 kDa), sodium poly(styrene sulfonate) (PSS) (nominal MWs of 177 kDa and 1.06 MDa), and poly(ethylene glycol) (PEG) (nominal MW of 600 kDa and 5 MDa). Figure 9 shows the narrow m/z range mass spectra of isolated (except for albumin) individual ions of MWs spanning nearly 2 orders of magnitude and a typical background noise spectrum. For acquisition of the data shown in Figure 9A–E, an individual ion from each sample was isolated with suspended trapping and repeated chirp excitation and detected in the m/z range covered by a 200-kHz (broadband) detection bandwidth. These experiments utilized the IonSpec transient digitizer and were limited to 256K data points (1.28 s). Figure 9F illustrates several discrete ions of the smallest compound studied which were isolated and detected to insure their positive identification due to the low S/N (2:1). In a typical experiment, multiple (5–20) individual ions were isolated and remeasured multiple times during which the chirp excitation amplitude (V_{pp}) was gradually increased. The number of ions decreased as ions were ejected from the cell with increasing cyclotron radii. The amplitude of the frequency-domain signal increases as V_{pp} is increased, and that with the maximum V_{pp} before the ejection of the ion(s) was taken as the maximum signal

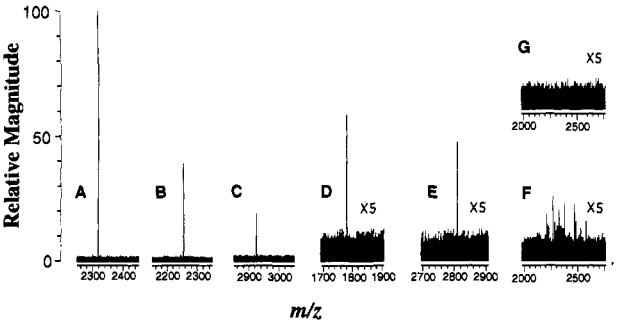

Figure 9. Several mass spectra of *individual* ions produced from molecules with MWs spanning nearly 2 orders of magnitude. Also presented in this figure is a mass spectrum demonstrating the typical background noise observed. All spectra shown in this figure were acquired with an analog-to-digital conversion rate of 200 kHz. FTICR mass spectra for individual ions for (A) a nominal 5-MDa PEG, (B) a nominal 1.06-MDa PSS, (C) a nominal 600-kDa PEG, (D) a nominal 177-kDa PSS, (E) bovine albumin dimer, (F) bovine albumin, and (G) the background in the corresponding m/z region for F. Background spectra in other m/z regions are qualitatively similar.

Table 2. Signal-to-Noise Ratio (S/N) from Experimental Measurement

sample	MW (Da)	m/z[a]	z[b]	S/N[c]
PEG (5 MDa)	5 000 000[d]	2300 ± 500	2200 ± 400	60 ± 20
PSS (1.06 MDa)	1 060 000[d]	2250 ± 500	470 ± 100	20 ± 5
PEG (600 kDa)	600 000[d]	2900 ± 500	205 ± 35	10 ± 3
PSS (177 kDa)	177 000[d]	1800 ± 500	100 ± 28	6 ± 2
bovine albumin dimer	133 000	2800 ± 300	60 ± 6	4 ± 1
bovine albumin	66 300	2200 ± 300	30 ± 3	2 ± 0.5

[a] m/z range within which S/N values were measured. [b] The range of calculated charges on individual ions. For the synthetic polymers, large uncertainties are expected due to the polydispersity of the samples. [c] Average results from measurements of 5–20 individual ions from >3 injections. [d] Nominal MW; large polydispersities are expected.

amplitude. The S/N values are measured directly from the magnitude mode frequency-domain signal peak height and the baseline noise. The measured S/N, evaluated m/z range, and the corresponding number of charges on individual ions are summarized in Table 2. For the smaller molecules studied, the S/N values are directly proportional to the number of charges on each ion, as expected. Interestingly, we have noted a deviation from linearity at higher MW, the origin of which is currently under investigation. The S/N of 2:1 obtained for bovine albumin with 30 charges essentially defines the lower limit for detection of individual multiply charged ions in this m/z range with the conditions employed. It is possible that extension to lower MWs could be obtained by formation and detection of lower m/z ions (i.e., higher charge states). For example, a 30-kDa protein at an m/z of 1000 will carry 30 charges and should be detectable as an individual ion. The limit of 30 charges may also be lowered by further improvement in preamplifier design, noise reduction, the acquisition of longer time domain signals, or operation at higher magnetic field strength.

Recently, Limbach et al.[29] measured the detection limit of a 3-T FTICR instrument for benzene molecular ions formed by electron ionization. They obtained a lower detection limit of 177 singly charged ions with a S/N of 3:1 under a well-defined set of experimental conditions. Due to the differences in instrumentation and detection conditions, it is difficult to draw a direct comparison between the two sets of results. Limbach et al.[29] have used a cyclotron radius that is 50% of the maximum allowed radius, a 1-s transient length, and heterodyne mode as the criterion for detection. In our experiment, cyclotron radii 90–95% of the maximum allowed radius are estimated as the signal magnitude was measured immediately prior the ejection of ions by increasing the chirp excitation V_{pp}. If we adjust our results to a S/N of 3:1 and allow a correction for differences in cyclotron radius and

transient length (1.28 s), we obtain an adjusted lower detection limit of ≈100 charges from this work. The remaining differences may be due to the difference in detection circuit capacitance, detection bandwidth (200-kHz broad band in this work vs heterodyne mode in their work), ion cyclotron frequency (40–60 kHz in this work vs 600 kHz in their work), and methods of signal amplification. It should be pointed out that in the case of individual multiply charged ions the coherent motion of the charge packet (required for the best signal magnitude and resolution) is guaranteed. The coherence of motion for an ensemble of ions (singly charged or not) will depend more heavily on space charge effects, spatial and kinetic energy distributions of ions before excitation, and the rate at which the ion cloud dephases due to collisions with background neutrals.

Conclusions

We have presented several types of evidence regarding the FTICR detection of very large multiply charged individual ions produced by ESI. The behavior of these ions when subjected to suspended trapping or increased excitation, as well as the requirement of greater gas pulses, either longer duration or higher peak pressure, to efficiently trap these species, distinguishes these ions from those of the large populations of smaller ions typically studied. Furthermore, the TRIC method has been introduced and used to demonstrate the stepwise frequency-shift behavior of cyclotron frequencies, which strongly supports their identification as individual ions. The possibility that even two ions would have the same cyclotron frequency (i.e., m/z) and would simultaneously undergo the same observed shifts is extremely remote. As an unexpected and surprising feature of this work, we found that some PEG ions can both increase and decrease the charge state during the observation period. The possible loss and reattachment of Na^+ ions during the acquisition of the time-domain signal is intriguing and clearly warrants further study. This observation highlights the fact that processes that occur with very small rates, and that would be difficult to see with large ion populations, become readily apparent for an individual ion that can be detected for extended periods. Similarly, the observation of individual ions should provide new insights into ICR processes, in particular, ion damping, the excitation of magnetron motion, and the study of Coulombic contributions through the study of the ion–ion interactions for two or more individual ions each having large charge.

Individual ion measurements should be even more beneficial for the study of smaller molecules if detection sensitivity can be further improved, and if even larger, more highly charged ions can be produced by ESI. On the basis of our studies to date, we see no reason to preclude the detection, mass determination, and reactive studies of substantially larger molecules. In addition, the TRIC technique affords the provision to monitor ion–molecule reactions of highly charged individual ions in "real time". Many fascinating possibilities for future studies involving ESI–FTICR and large molecules are also evident. For example, this technique may provide the unique ability to directly measure the excited-state lifetimes after photoactivation of large molecules with FTICR mass spectrometry, as well as provide a direct correlation between precursor and product ions, thus elucidating photodissociation pathways. Improvements in sensitivity will serve to further the capabilities by allowing fewer charges, and thus smaller molecules, to be probed. The present estimate of the minimum number of charges required for detection, based on the measurements reported here, is around 30 for acquisition periods of 1.28 s. Lower noise detection circuitry and longer acquisition periods could substantially reduce this. The TRIC technique may eventually lead to an entirely new form of "real time" ion monitoring, routinely providing $(MS)^n$ information from a single acquisition. Finally, the new capabilities of accurate MW determination for large molecules should be significant to a number of research areas including the characterization of large synthetic polymers and microparticles, DNA mapping through the mass measurement of restriction fragments, and the study of biomacromolecular systems including higher order structures involving assemblies of proteins, nucleic acids, and membranes.

Acknowledgment. This research was supported by internal PNL exploratory research and the Director, Office of Health and Environmental Research, U.S. Department of Energy. Pacific Northwest Laboratory is operated by Battelle Memorial Institute for the U.S. Department of Energy, through Contract DE-AC06-76RLO 1830. We thank Drs. A. L. Rockwood, Ruidan Chen, and Steven Van Orden for helpful comments and suggestions.